A discrete S=1 model for electron localization properties of the mixed-valence biferrocenium salts

1993 J. Phys.: Condens. Matter 5 469

(http://iopscience.iop.org/0953-8984/5/4/014)

J. Phys.: Condens. Matter 5 (1993) 469–476. Printed in the UK

A discrete $S = 1$ model for electron localization properties of the mixed-valence biferrocenium salts

K Boukheddaden†, J Linares†, S Galam‡ and F Varret†

† Département de Recherches Physiques, Laboratoire associé au CNRS (UA 71) et à l'Université Pierre et Marie Curie, Tour 22, 4 place Jussieu, 75252 Paris Cédex 05, France

‡ Groupe de Physique des Solides, Laboratoire associé au CNRS (UA 17) et aux Universités Paris VII et Pierre et Marie Curie, Tour 23, 2 place Jussieu, 75251 Paris Cédex 05, France

Received 30 July 1992

Abstract. The peculiar biferrocenium cation configurational diagram is discretized in terms of a fictitious spin $S = 1$. At the solid state, this leads to a Blume–Emery–Griffiths Hamiltonian which is solved in the mean-field approach. Order–disorder transitions are obtained, either continuous or discontinuous, together with a thermal equilibrium between trapped and delocalized states. These features are discussed with respect to characteristics of the measuring techniques.

1. Introduction

The biferrocene molecule is a dimer made of equivalent ferrocene (Fe^{II}) moieties A, B (figure 1). Under monoelectronic oxidation, the resulting biferrocenium cation possesses inhomogeneous formal oxidation states Fe^{II}, Fe^{III}. The impaired electron can either occupy a symmetric bonding orbital (this is the 'delocalized state') or be trapped in any of the moieties (this is a 'localized state') with a concommitant asymmetric distortion of the molecule corresponding to a decrease of the Fe–Cp distance by ~ 0.025 Å [1–3]. We emphasize that we are using the terminology 'localized–delocalized' in the context of molecular states without connection to insulative–conductive properties of the solid state. The most comprehensive model for molecular mixed valences is that of PKS [4–6] which involves one orbital on each moiety. It is based on the competition between following three energy terms:

(i) the elastic energy associated with the asymmetric distortion;

(ii) the vibronic coupling between electronic energy and asymmetric distortion: this leads to different equilibrium positions when the electron is trapped in moiety A or in moiety B.

(iii) the electronic interaction between the moieties, i.e. transfer integral, originating from the chemical bonding between moieties.

PKS model is adequately visualized, in the Born–Oppenheimer approach, by a configurational diagram (figure 2) which provides a qualitative discussion of electron transfer: for instance, a small (large) value of the transfer integral, associated with a small (large) gap on the configurational diagram, leads to a slow (fast) electron

0953-8984/93/040469+08$07.50

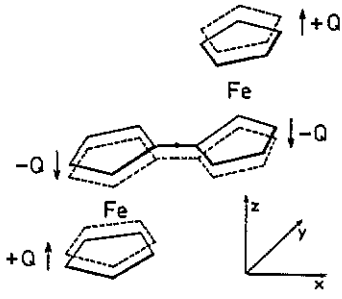

Figure 1. Schematic view of the biferrocenium cation and its asymmetric distortion Q_-; note the mirror symmetry with respect to the figure plane.

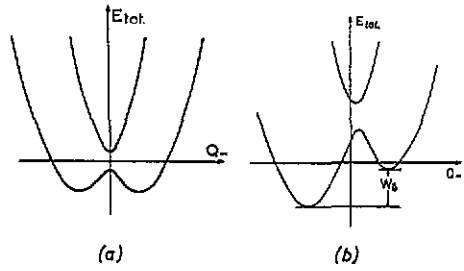

Figure 2. Configurational diagrams, i.e. adiabatic energy curves against Q_- in the *simple* PKS case, assuming a weak transfer integral: (*a*) symmetric external potential (*b*) asymmetric external potential which traps the mixed valence.

transfer and an easy (difficult) electron trapping under the effect of an external asymmetric potential.

In the solid state, as suggested by Dong *et al* [2], intermolecular interactions can be expressed through such an asymmetric potential depending on the distortion of neighbouring molecules. Then, in the limit of small values of the transfer integral, the problem may be discretized in terms of a fictitious spin $\frac{1}{2}$, with eigenvalues $\pm\frac{1}{2}$ corresponding to the trapped states on each moiety, and an iteraction term of Ising type

$$\hat{\mathcal{H}} = \sum_{(i,j)} J_{ij}\hat{\sigma}_i\hat{\sigma}_j . \tag{1}$$

These spins $\frac{1}{2}$ are used to make the analysis more tractable and bear no relation to true spins. Resolution of this Hamiltonian in the mean-field approach leads to a second-order, order–disorder transition. Such a model describes adequately the 'fusion type' behaviour of the Mössbauer spectra of di-ethyl substituted biferrocenium I_3^- [7,8] (as discussed in section 6, the electron transfer is fast at Mössbauer timescales, so that the spectra reflect thermally averaged properties).

However, due to the peculiarity of the MO scheme of the biferrocenium cation involving two orbitals on each moiety [9, 10] an extension of the models is needed. This leads to the present 'extended PKS model', the vibronic analysis of which will be presented elsewhere [11]. Here, to outline the possible consequences of this extended model, we present a crude treatment performed at the discrete level.

2. Peculiarity of the biferrocenium cation

A major problem is the determination of both the type and the multiplicity of molecular orbitals which can represent [12] the electronic functions of PKS model. The difficulty comes from the a_{1g}/e_{2g} inversion [13, 14] between ferrocene and ferricinium MO schemes (figure 3). We resolved this problem using computations of the Mössbauer quadrupole splitting, performed in the MO approach [9, 10, 15] (SCC

X_α method): a a_{1g}-based HOMO would result in a quadrupole splitting increased with respect to that of biferrocene; this is not the case in any of the biferrocenium salts studied so far (see [16] for a review of biferrocenium salts). In contrast, MO schemes with an e_{2g}-based HOMO lead to computed quadrupole splittings in excellent agreement with experimental data ($\simeq$ 0.5–1 mm s^{-1}). Then, a HOMO belonging to the fourfold space $d^A_{xy} \otimes d^A_{x^2-y^2} \otimes d^B_{xy} \otimes d^B_{x^2-y^2}$ must be considered, and this increases the dimensionality of the PKS problem: in the static approach, the PKS matrix is now 4×4 (instead of 2×2), and the configurational diagram (figure 4) displays four curves instead of two. This is the *'extended PKS model'*.

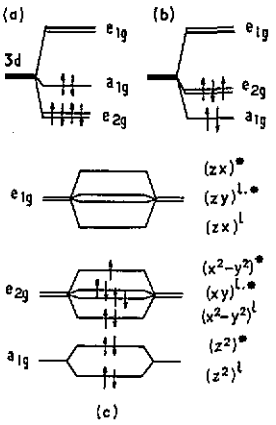

Figure 3. Molecular orbital energy scheme of (*a*) ferrocene, (*b*) ferricinium, (*c*) biferrocenium, neglecting the low-symmetry ligand field and in the absence of molecular distortion. The Cartesian expression of the orbitals is relative to the set of axes shown in figure 1.

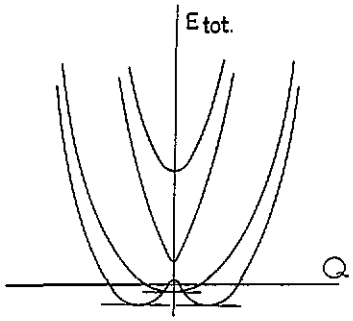

Figure 4. Configurational diagram in the *extended* PKS case, in the absence of asymmetric external potential, and its discretization.

A detailed investigation of intramolecular properties, in the full vibronic treatment of the 'extended PKS model', will be published in [11]: the respective roles of transfer integrals, vibronic couplings and low-symmetry ligand field will be discussed and calculations of electron transfer rates will be also reported.

It should be noted that the transfer integral takes on rather different values according to the nature of orbitals: in the case of *mirror symmetry* (with respect to the figure plane of figure 1), which is considered here for simplicity, there is no mixing between the $d^A_{xy} \otimes d^B_{xy}$ and $d^A_{x^2-y^2} \otimes d^B_{x^2-y^2}$ subspaces; the transfer integral in the d_{xy} subspace is much smaller than that of the $d_{x^2-y^2}$ subspace (because the former orbitals are odd with respect to the mirror plane and do not interact with the p_z orbitals of the bridge). Then the configurational diagram is made up of two uncoupled 'usual' PKS diagrams, one of which (d_{xy}) enables easy electron trapping, while the second one is typical for electronic delocalization with more difficult electron trapping. The vibronic treatment of intramolecular properties of biferrocenium has been reported in [16].

The general description of solid-state properties requires one to consider N vibronic oscillators as described above, and to introduce intermolecular interactions through asymmetric potentials. We are currently dealing with the full vibronic

treatment of the problem, either for a small number of interacting molecules, or for an infinite lattice treated in the mean-field approximation. Here we use a discrete-level approach in the mean-field treatment.

Such a discrete approach of the problem, although very crude, allows one to predict a large variety of thermodynamic behaviours which have been observed experimentally [17], but up till now lacked a comprehensive theoretical description.

3. Schematization of intramolecular properties

Since the height of the barrier of the double-well curve is $\simeq 300\ \mathrm{cm}^{-1}$ [16] and the gap between the single-well curve and the corresponding excited curve is certainly larger, it is reasonable to consider only the lowest curve of each pair of PKS curves.

The double-well curve is then treated as a two-level system, whose degeneracy can be lifted by the external asymmetric potential. On the other hand, the single-well curve is much less sensitive to the asymmetric potential (the same distortion requires an external potential $\simeq 50$ times larger for $d_{x^2-y^2}$ orbitals than for d_{xy} [16]), and is adequately represented by a singlet state (figure 4).

However, vibrational degeneracy associated with the single-well curve is clearly larger than that of the 'bottom states' of the double well. This is roughly accounted for by giving the singlet a two-fold degeneracy. Owing to the roughness of the present modelization there is no point further refining this degeneracy ratio.

These features are adequately accounted for by a fictitious spin $S = 1$, with an 'extra' degeneracy $g_0 = 2$ of the $S_z = 0$ state.

4. The Hamiltonian

Interacting $S = 1$ systems have been used in the Blume–Emery–Griffiths [18] Hamiltonian (introduced to describe ^{3}He–^{4}He properties).

$$\hat{\mathcal{H}} = -\sum_{(i,j)} J_{ij}\hat{\sigma}_i\hat{\sigma}_j - \sum_{(i,j)} K_{ij}\hat{\sigma}_i^2\hat{\sigma}_j^2 - \sum_i \Delta_i\hat{\sigma}_i^2 \qquad (2)$$

where $\hat{\sigma}_i$ is the projection of the ith spin on the quantization axis. Eigenvalues of $\hat{\mathcal{H}}$ are $\sigma_k = 0, \pm 1$, in agreement with previous section. All contributions to equation (2) are indeed relevant to the mixed-valence problem:

$-\Delta_i\hat{\sigma}_i^2$ expresses the energy difference between the singlet and doublet of the isolated ith molecule; it originates from the intra-molecular low-symmetry ligand field. It is a single-spin symmetry breaking field;

$-J_{ij}\hat{\sigma}_i\hat{\sigma}_j$ is a contribution to the pair energy which lifts the degeneracy of the doublet states by spontaneous symmetry breaking;

$-K_{ij}\hat{\sigma}_i^2\hat{\sigma}_j^2$ is a second contribution to the pair energy, which does not lift the degeneracy of the doublet.

Both interaction terms (J, K) are due to the intermolecular crystal field; they have different symmetries: the J-term breaks the inversion symmetry of the molecule, whereas the K-term does not, and merely adds up to the intramolecular low-symmetry ligand field. It must be noted that the J-term alone is responsible for electron trapping.

Formally, equation (2) describes an $S = 1$ Ising-like model with anisotropy (Δ term).

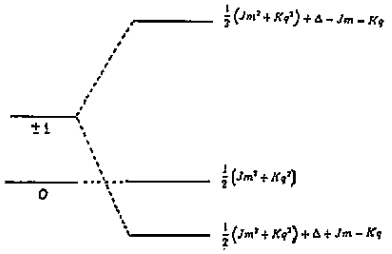

Figure 5. Energy scheme of the fictitious spin in the mean-field approach.

5. Mean-field treatment

We have treated equation (2) in the mean-field approach, assuming all molecules to be identical, in the case of a 'ferromagnetic' J-interaction (which favours an 'in-phase' valence trapping in the solid state). The case of an 'antiferromagnetic' J-coupling would only require dealing with two 'out-of-phase' sublattices.

The mean-field treatment of the ferromagnetic case leads one to define two order parameters (using the same notations as [18]):

$$m = \langle\hat{\sigma}\rangle q = \langle\hat{\sigma}^2\rangle \tag{3}$$

and the various terms of the Hamiltonian become

$$\sum_i \Delta_i \hat{\sigma}_i^2 (\text{unchanged}) \tag{4}$$

$$\sum_{(i,j)} J_{ij}\hat{\sigma}_i\hat{\sigma}_j = J\sum_i (\hat{\sigma}_i\langle\hat{\sigma}\rangle - \tfrac{1}{2}\langle\hat{\sigma}\rangle^2) \tag{5}$$

and,

$$\sum_{(i,j)} K_{ij}\hat{\sigma}_i^2\hat{\sigma}_j^2 = K\sum_i (\hat{\sigma}_i^2\langle\hat{\sigma}^2\rangle - \tfrac{1}{2}\langle\hat{\sigma}^2\rangle^2) \tag{6}$$

where the second terms in the brackets account for 'self-consistent' terms. Here J and K include the number of first neighbours ($J = zJ_{ij}$, $K = zK_{ij}$).

The Hamiltonian may be written as the sum of one-site Hamiltonians:

$$\hat{\mathcal{H}} = \tfrac{1}{2}(Jm^2 + Kq^2) + \Delta\hat{\sigma}^2 - Jm\hat{\sigma} - Kq\hat{\sigma}^2 \tag{7}$$

whose eigenstates are $\sigma = \pm 1, 0$, with eigenvalues (shown in figure 5)

$$E(\sigma = 1) = \tfrac{1}{2}(Jm^2 + Kq^2) + \Delta - Jm - Kq \tag{8}$$

$$E(\sigma = 0) = \tfrac{1}{2}(Jm^2 + Kq^2) \tag{9}$$

and,

$$E(\sigma = -1) = \tfrac{1}{2}(Jm^2 + Kq^2) + \Delta + Jm - Kq. \tag{10}$$

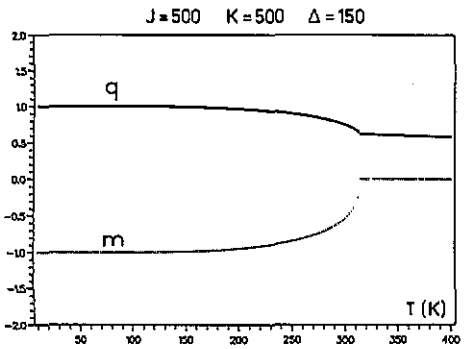

Figure 6. Second-order order–disorder transition, resulting from the set of values: $J = K = 500$ K, $\Delta = 150$ K.

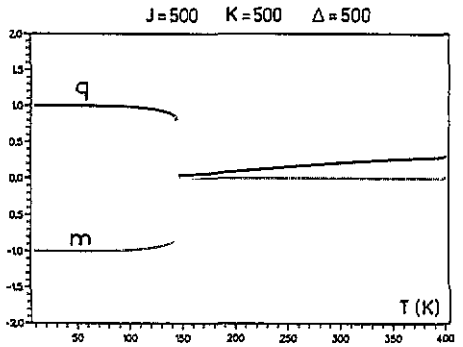

Figure 7. First-order order–disorder transition, resulting from the set of values: $J = K = \Delta = 500$ K.

The partition function Z and the free energy $F = -k_B T \ln(Z)$ are derived giving

$$Z = (2 + 2e^{\beta(Kq-\Delta)} \cosh(\beta J m)) \exp(-\tfrac{1}{2}\beta(Jm^2 + Kq^2)) \tag{11}$$

and,

$$F = \tfrac{1}{2}(Jm^2 + Kq^2) - k_B T \ln(2 + 2e^{\beta(Kq-\Delta)} \cosh(\beta J m)) \tag{12}$$

where $\beta = 1/k_B T$.

Minimization of F with respect to m and q leads to the coupled system

$$m = 2e^{\beta(Kq-\Delta)} \sinh(\beta J m)/2 + 2e^{\beta(Kq-\Delta)} \cosh(\beta J m) \tag{13}$$

and

$$q = 2e^{\beta(Kq-\Delta)} \cosh(\beta J m)/2 + 2e^{\beta(Kq-\Delta)} \cosh(\beta J m). \tag{14}$$

From equations (13) and (14) several solutions in m and q are obtained. Corresponding values of the free energy are then computed numerically in order to select at each temperature the thermodynamically stable solution.

6. Results

According to the values of the coupling parameters J, K and low-symmetry ligand field Δ, three typical situations are obtained. Corresponding figures (6–8) are easily interpreted by noting that m denotes the degree of valence trapping, and q is the relative population of localized states.

(i) Figure 6: order–disorder transition of second order; it can be obtained in cases of well isolated d_{xy} ground state, leading to the simple PKS case.

(ii) Figure 7: order–disorder transition of first order; it requires a tight thermodynamic competition between d_{xy} and $d_{x^2-y^2}$ orbitals (such as all three states are thermally accessible), associated with a large coupling parameter K.

(iii) Figure 8: progressive conversion from trapped to delocalized, it occurs for weak coupling parameters.

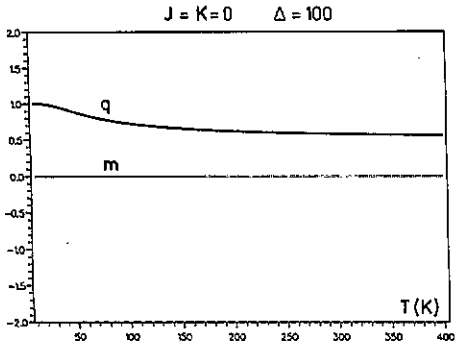

Figure 8. Thermal progressive conversion from trapped to delocalized, resulting from the set of values: $J = K = 0$, $\Delta = -100$ K.

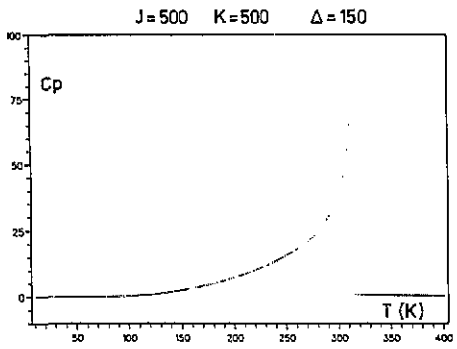

Figure 9. Specific heat C_p (in J mol^{-1} K^{-1}) computed with the set of parameters of figure 6., versus temperature (K).

We have not investigated *thoroughly* the corresponding phase diagram; however, the following basic features have been outlined:

(i) the order–disorder transition occurs when the ground state at 0 K belongs to the doublet $\sigma = \pm 1$; this requires $J \neq 0$ (> 0) and $J > \Delta - K$.

(ii) the second-order transition turns to first order when all three states are thermally accessible ($J - \Delta + K \simeq kT$), with a sufficiently large value of K.

Thermal effects associated with these evolutions have been calculated, and will be discussed in next section.

7. Discussion

Comparison with experimental data is discussed here in terms of calorimetric, structural and spectroscopic measurements:

(i) specific heat measurements: we have calculated the $Cp(T)$ curve corresponding to the second-order transition (figure 9). A λ-shaped anomaly is obtained, as expected, but it is rather small and seems hardly detectable; this is mainly because we only consider the entropy change associated with the onset of disorder ($R \ln 2 = 5.76$ J K^{-1} mol^{-1}). This value might be modified by the vibrationnal contributions; the vibronic treatment of the problem which is in progress should clear up this point.

(ii) structural studies: the x-ray diffraction technique is sensitive to spatial average of the distortion. So, despite fast measuring frequency, it can only detect the order parameter m (it is worth noting that m is an average over all states, and differs from the average performed over the double-well shaped curve alone).

(iii) spectroscopic measurements: the observed spectra essentially depend on the measuring frequency of the technique, compared to electron transfer rates in the system. It is clear from both experimental data [17] and recent vibronic calculations that the transfer rate between the two wells of the double-well curve is faster than the Mössbauer measuring frequency (which is $\sim 10^8$ s^{-1}): therefore the Mössbauer spectra are sensitive to the average distortion, i.e. to the order parameter m. This

basically explains the 'fusion-type' behaviour reported by Sano *et al* [7, 8]. The converse also holds: a fast technique such as IR, which is faster than the electron transfer rate in most cases [16], will reveal a trapped state at all temperatures.

However, relaxation rates between the d_{xy} and $d_{x^2-y^2}$ orbitals are not known; it seems that these rates might be smaller than the Mössbauer frequency in some cases where the Mössbauer reveal the coexistence of components typical for trapped and delocalized states over a large temperature range. Then, the order parameter q exactly represents the surface ratio of the trapped component. On the other hand, fast relaxation rates should mix together the trapped and delocalized components, and prevent one from measuring q in such a case. The various features reported here have been experimentally observed [17], depending on the nature of the counter-anion, of the packing, and also on eventual substituents on the cyclopentadienyl-rings. The present parameters J, K, Δ are found to change considerably from one complex to another.

8. Conclusion

The crude approach presented here has outlined the various possibilities offered by an extension of the PKS model which accounts for the actual multiplicity of the HOMO of the biferrocenium cation. A more refined description requires a vibronic treatment of the model, which is in progress. Further comparisons to experimental data are required to quantify intermolecular interactions as well as the low-symmetry ligand field of the molecule.

Acknowledgments

We are indebted to J Y Saillard and J P Launay for helpful discussions.

References

[1] Dong T Y, Hendrickson D N, Pierpont C G and Moore M F 1986 *J. Am. Chem. Soc.* **108** 963–71
[2] Dong T Y, Kambara T and Hendrickson D N 1986 *J. Am. Chem. Soc.* **108** 4423–32
[3] Konno M, Hyodo S and Iijima S 1982 *Bull. Chem. Soc. Japan* **55** 2327–35
[4] Piepho S B, Krausz E R and Schatz P N 1978 *J. Am. Chem. Soc.* **100** 2996–3005
[5] Wong K W and Schatz P N 1981 *Prog. Inorg. Chem.* 369–449
[6] Wong K W and Schatz P N 1981 *Chem. Phys. Lett.* **71** 152–7
[7] Nakashima S and Sano H 1989 *Chem. Lett.* 1075–8
[8] Nakashima S, Nishimori A, Masuda Y, Sano H and Sorai M 1991 *J. Phys. Chem. Solids* **52** 1169–80
[9] Rabah H 1989 *Thèse de Doctorat* University of Le Mans, France
[10] Varret F, Rabah H, Guillin J and Talham D 1991 *Mixed Valence Systems: Applications in Chemistry, Physics and Biology (NATO ASI Series)* ed K Prassides (Dordrecht: Kluwer) pp 359–64
[11] Boukheddaden K, Linares J and Varret F to be published
[12] Piepho S B 1988 *J. Am. Chem. Soc.* **110** 6319–26
[13] Collins R L 1965 *J. Chem. Phys.* **49** 1072–80
[14] Prins R 1970 *Mol. Phys.* **19** 603–20
[15] Rabah H, Guillin J, Cereze-Ducouret A, Greneche J M, Talham D, Boukheddaden K, Linares J and Varret F *Hyperf. Interact.* at press
[16] Boukheddaden K, Linares J, Bousseksou A, Nasser J, Rabah H and Varret F *Chem. Phys.* at press
[17] Hendrickson D N 1990 *Mixed Valence Systems: Applications in Chemistry, Physics and Biology (NATO ASI Series)* ed K Prassides (Dordrecht: Kluwer) pp 67–90
[18] von Hintermann A and Rys F 1969 *Helv. Phys. Acta* **42** 608
Blume M, Emery V J and Griffiths R B 1971 *Phys. Rev.* A **4** 1071–7